

Lecture on Orbits in the Strong Focussing Synchrotron

(Delivered at Saclay 21st May, 1953)

J. B. Adams F. K. Goward

CERN/PS/JBA-FKG 1.

1. Introduction

The highest energy which has so far been achieved by a proton accelerator is about $2\frac{1}{2}$ GeV (2.5×10^9 eV) from the Brookhaven Cosmotron. In this machine particles are accelerated along an orbit of radius about 10 metres inside a vacuum chamber whose available aperture is about 70 cm. x 15 cm.. The cost of such a conventional synchrotron is 6 to 10 million dollars and using the same kind of techniques it would become very costly to extend the energy to 10 GeV. Some thought was given by C.E.R.N. to such an extension in early 1952 and a figure of about 15 million dollars was then estimated, provisionally, as the likely cost of a 10 GeV 'conventional' machine.

Some fundamental change in technique is desirable for higher energy machines and this lecture will describe such a change, first suggested by Courant, Livingston and Snyder* and since then extended and modified by work in both Europe and U.S.A.. The C.E.R.N. laboratory is planning a 'strong-focussing synchrotron' of this type to give energies of 20-30 GeV.

In this lecture the conventional and strong-focussing methods will be compared and the developments in the strong-focussing method described, recalling first the essential principles of conventional focussing and then proceeding to the later developments. In this lecture only the motion of particles circulating at constant energy in static magnetic fields is considered. No problems associated with oscillations of the particles in energy or phase due to acceleration are included.

2. The Conventional Synchrotron

The focussing principle of a conventional synchrotron relies on two fundamental ideas:

- (a) To give axial stability the axial field, which bends the particles to the required circle, must decrease as the radius increases. Such a condition

* Phys. Rev. 88, 5, 1190, December 1952.

is necessary in order to produce the outward 'bowing' of the field lines required to return a particle to the median plane (See fig. 1a).

(b) To give radial stability the rate of decrease of field with radius must be limited. The limit is shown by considering a particle of energy E_0 injected tangentially into a field at two different radii, r and r_0 . The limit of zero focussing occurs when the particles simply maintain their radii i.e. when $H_z r = H_0 r_0$ or $H_z = H_0 (r/r_0)^{-1}$. To obtain positive radial focussing of the particles towards a stable orbit at r_0 the axial field at r must be greater (for $r < r_0$) than that given by the above condition i.e.

$$H_z = H_0 (r/r_0)^{-n} \text{ with } n < 1.$$

The condition for both axial and radial stability to coexist, therefore, is that

$$H_z = H_0 (r/r_0)^{-n} \text{ with } 0 < n < 1 \quad \dots \dots \dots (1)$$

To obtain more quantitative information about the orbits the axial field, H_z , is approximated, putting $r - r_0 = \rho$, by the relationship

$$H_z = H_0 (1 - n\rho/r_0) \dots \dots \dots (2)$$

from which the radial field component is approximately

$$H_r = - H_0 n \rho / r_0 \dots \dots \dots (3)$$

For such a 'linear' field motion is obtained which is, to a first approximation, independent in the axial and radial directions. Some coupling occurs in the second approximation because the machine is circular and there are consequent centrifugal terms in the equations of motion; in addition strictly linear fields radially and axially cannot coexist in a three dimensional machine. These factors will, however, be neglected and the equations of motion written:

$$\ddot{\rho} = - \omega_0^2 (1-n)\rho, \quad \dots \dots \dots (4a)$$

$$\ddot{z} = - \omega_0^2 n z \quad \dots \dots \dots (4b)$$

with solutions:

$$\rho = a \cos \omega_0 (1-n)^{\frac{1}{2}} t + b \sin \omega_0 (1-n)^{\frac{1}{2}} t, \quad \dots \dots \dots (5a)$$

$$z = c \cos \omega_0 n^{\frac{1}{2}} t + d \sin \omega_0 n^{\frac{1}{2}} t \quad \dots \dots \dots (5b)$$

In these equations the angular frequency of rotation, $d\theta/dt$, of the particle is denoted by ω_0 and a, b, c, d are constant determined by the injection conditions.

The condition for simultaneous stability in both θ and z directions, $0 < n < 1$, follows from equation (5). Typical orbits for the radial motion are shown in Fig. 2. For equal focussing action in both directions $n = 0.5$ and particles originating in a point focus refocus after about 0.7 revolutions, the focussing or betatron wavelength being $\sqrt{2}$ circumferential lengths.

The first consideration in designing a synchrotron is to fix on the minimum aperture required. Such consideration will first be restricted to a machine whose magnetic field has no irregularities such as those which might arise from mechanical and electrical defects. Only the aperture required to accommodate the focussing oscillations, and not synchrotron oscillations will be studied. The aperture, A , required is then proportional to the angular spread, ϕ , of the source, or to some effective angular spread resulting from collisions with residual gas, and to the focussing wavelength, λ , that is

$$A \propto \phi \lambda, \dots \dots \dots (6)$$

assuming that the source occupies a definite small fraction of the apert. Starting from a given injector and using focussing devices to bring the source size to the required constant fraction of the donut aperture, kA , the angular spread of the source is, with optimum adjustment, inversely proportion to the size of the aperture, that is:

$$\phi \propto A^{-1} \dots \dots \dots (7)$$

This follows from the Helmholtz Lagrange condition in an optical system.

From the equations (6) and (7)

$$A \propto \lambda^{\frac{1}{2}} \dots \dots \dots (8)$$

It is desirable, therefore, to reduce the focussing wavelength, λ , to a small value as shown in fig. 3. Such a reduction is possible in, say, the radial direction by making n take large negative values, when the radial aperture, A_{θ} , varies with n according to the relationship

$$A_{\theta} \propto n^{-\frac{1}{4}} \dots \dots \dots (9)$$

since the wavelength is inversely proportional to $n^{\frac{1}{2}}$ (see equations 5).

These n values would, however, give defocussing in the axial direction, the behaviour corresponding to the orbit marked '+' in figure 2, with z replacing as the ordinate scale. From equation (9) the advantages, from the viewpoint of radial aperture limitation, of reducing the radial focussing wavelength are

quite clear but no practical way of achieving a reduction in both the axial and radial apertures simultaneously was advanced for some time. The suggestion made by Courant Livingston and Snyder is important because it does offer this possibility. It ensures a variation of aperture with field gradient of the form

$$A \propto n^{-\frac{1}{2}} \quad \dots \quad (10)$$

where A now refers to both radial and axial apertures.

3. The Strong Focussing Synchrotron

Courant, Livingston and Snyder showed that focussing may be obtained in both radial and axial directions simultaneously if the magnet circumference is broken up into a number of sectors, N, with alternating large positive and negative values of n. The scheme may be illustrated by plots of some typical orbits, in both directions, as shown in fig. 4. This figure is drawn for the case in which the field gradient (or n value) and sector length are so related that a phase change of $\pi/2$ occurs in the normal betatron oscillation occurring in one focussing sector. These orbits are special cases of focussing oscillations in which repetition occurs in an integral number of sectors, but for a machine which is perfectly constructed there is a continuous range of values of n for which stable operation in both directions is possible. This stable region is shown in fig. 5., where the n values for the ^{negative} ~~positive~~ gradient sectors, n_2 , are not necessarily equal to the n values for the positive gradient sectors, n_1 . The limits of the stable region are found by a simple application of Floquet's theorem which states that, in problems of this type, solutions can be found which are merely multiplied by an exponential factor, $e^{\pm i\mu}$, in passing from one unit to the next, the unit consists of two sectors in this particular problem. Using this theorem, stable operation is possible provided that μ is real, when the factor $e^{\pm i\mu}$ is oscillatory. μ then corresponds to the phase shift between each pair of sectors, the phase being measured in terms of the focussing wavelength in the new composite system. Quantitatively the condition for stability is,

$$|\cos \mu| > 1 \quad \dots \quad (11)$$

$$\text{where } \cos \mu = \cos \gamma_1 \cosh \gamma_2 - \frac{1}{2} \left(\frac{\gamma_1}{\gamma_2} - \frac{\gamma_2}{\gamma_1} \right) \sin \gamma_1 \sinh \gamma_2 \quad \dots \quad (11)$$

$$\gamma_1 = 2\pi n_1 \frac{1}{2} / N \text{ and } \gamma_2 = 2\pi (-n_2) \frac{1}{2} / N \quad \dots \quad (11)$$

(remember that n_1 is a positive number and n_2 a negative number).

Some typical orbits (in the median plane) both inside and outside the stable region are shown in fig. 6, the machine being normally operated at some point on the diagonal of figure 5 to give equal stability radially and axially.

The orbits inside the stable area consist, approximately of long period sinusoidal oscillations with other oscillations superposed of wavelength equal to two sectors lengths (figs. 6a and 6b). The relative magnitude of these superposed oscillations decreases as we operate at points increasingly close to 0 in fig. 5 and there is thus some advantage to be gained, in reduction of aperture for given injection conditions, by operating the synchrotron rather nearer to 0 than is the case in the ' $\pi/2$ mode' of fig. 4. The mode number, μ , is defined as the phase change in a pair of sectors. This phase change is defined in terms of the focussing oscillation in the composite system and not in terms of the betatron oscillation in a single focussing sector. The mode used will depend on a compromise between the focussing and synchrotron oscillation amplitudes, but operation with a mode number as low as the $\pi/5$ mode is quite likely. (In this mode the oscillation will repeat every 20 sectors).

At the limits of the stable region the oscillation amplitude builds up linearly (fig. 6c); this situation will clearly arise since a linear rise must form the boundary between focussing behaviour (sinusoidal envelope) and defocussing (exponential envelope) behaviour. A special orbit could have been drawn on fig. 6(c), which maintained constant amplitude, by making the orbit originate at a radial position r_0 in the centre of a defocussing sector. Finally fig. 6(d) shows an orbit outside the stable region.

The ideal geometrical arrangement so far studied will certainly not be used in practice for various reasons. First it is necessary to have some separation between sectors having positive and negative n values, for both mechanical and magnetic reasons. Next it is necessary to put breaks in the magnet every so often to accommodate the R.F. accelerators, the injection mechanism, and other devices. Then again, the sectors can only be constructed and aligned within certain dimensional tolerances and variations are sure to exist in the magnetic properties of the iron used at different points of the circumference. All these factors introduce irregularities in the magnetic field which have important effects on the particle orbits as is shown in the next section.

4. Azimuthal Inhomogeneities

The operation of the strong-focussing synchrotron is very sensitive to irregularities in the geometrical alignment of the sectors, so this type of azimuthal inhomogeneity will be studied as a first example. The strong-focussing synchrotron is much more sensitive to alignment errors than a conventional machine, as is illustrated by the orbits plotted in fig. 7, where each type of machine is assumed to be manufactured accurately except for the displacement of δ , of a given small element of the circumference of length d . For convenience it has been assumed that the focussing oscillations are sinusoidal of wavelength λ although, as explained in Section 3, other smaller-wavelength oscillations are superposed. The displaced element, which is assumed short compared with λ , deflects the particle through an angle that depends on the error in magnetic field on the particles' orbit. The error in magnetic field depends on the displacement of the element, δ , and on the field index, n . As has been shown previously λ is inversely proportioned to $n^{\frac{1}{2}}$ so finally the angle of deflection, for a given displacement of the element, is inversely proportioned to λ^2 . The corresponding amplitude of oscillation induced by the displaced element is proportional to λ and to the angle of deflection, and is therefore ultimately proportional to $\frac{1}{\lambda}$, or to $n^{\frac{1}{2}}$. For element lengths of $\lambda/4$ the oscillation amplitude reaches a value in excess of $2f$, the value depending on the mode number and on whether the displaced element is focussing or defocussing.

If all individual elements in the circumferential length are displaced from the true circle in a random manner then the R.M.S. oscillation induced per revolution is \sqrt{S} times the R.M.S. displacement of a single element, where S is the number of elements. It is permissible to treat the irregularities as one 'effective' discontinuity (consisting approximately of the addition of a definite slope to the orbit) located at some point on the circumference.

In the strong focussing synchrotron the oscillation, already large, induced in one revolution can be further increased by resonant build-up of oscillations. This possibility exists as soon as the focussing wave-length becomes less than one circumferential length and is therefore not present in the conventional machine (see fig. 7). The resonance occurs when Q , the number of focussing oscillations per revolution, is integral, as is illustrated in fig. 8a, where the misalignment

is represented by the constant change in slope, \dot{Q} . The oscillation amplitude is seen to build up linearly. If the machine is operated well away from a resonance, however, the oscillation amplitude builds up until there is a reversal in the phase of the discontinuity relative to the focussing oscillation. For half integral values of Q the maximum amplitude reached is just that corresponding to the discontinuity acting once on the orbit, since the amplitude added in one revolution is immediately removed by the out-of-phase action in the subsequent revolution.

The amplitude of oscillation built up is most conveniently deduced as a function of Q from the construction shown in fig. 8b. This diagram shows the only closed orbit, along which a particle can circulate for many revolutions, with one slope discontinuity, \dot{Q} per revolution. There is only one amplitude corresponding to each λ or Q value which will give the required change in derivative, \dot{Q} , for the closed orbit, to repeat each revolution. All other orbits are formed by focussing oscillations of constant amplitude about this stable orbit and these will not repeat each revolution. The amplitude of this closed orbit may be plotted against Q as shown in fig. 8c. Although the closed orbit only becomes infinite for Q integral, for all practical purposes those values of Q are not permissible at which the amplitude of the closed orbit exceeds the donut dimensions. This range of Q values is shown as a 'forbidden band' in figure 8(c). The effect of the inhomogeneity is best represented by plotting the forbidden regions on a stability diagram of the type shown in fig. 5. There are, of course, forbidden Q values for both the radial and axial motions and the resulting stability diagram therefore takes the form shown in figure 9; the diagram is broken into $N/4$ separated usable bands in each direction, where N is the total number of sectors both focussing and defocussing.

Another particularly simple and instructive type of inhomogeneity met with in the strong focussing synchrotron occurs as a result of introducing straight field-free sections. These sections may be introduced intentionally and regularly for mechanical or electrical reasons. In addition, however, errors may be made in cutting all sectors to the same length or in adjusting their circumferential positions. Such errors may be considered formally as the random introduction of further straight sections.

The effect of straight field-free sections included regularly between positive and negative gradient sectors is merely to change the overall size of the stable area of fig. 5 since their presence does not alter the basic idea of a number of similar units following each other. With straight sections the unit is (0, +, 0, -), rather than (+, -), where 0 is used to represent a field free sector. A typical change caused by introducing field-free sectors is shown in fig. 10(a). If, however, we have only one field-free region in the circumferential length the unit of repetition is not one single (+, -) unit but rather the whole circumference of the machine, consisting of $N/2$ such units. The stability diagram is then split into $\frac{N}{2}$ stable bands corresponding to each direction, radial and axial, as shown in figure 10(b). This is double the number of bands (per direction) obtained with the simple misalignment of figure (9). The difference arises because build-up of the oscillation amplitude due to a misalignment inhomogeneity is not possible for half integral values of Q , since the effect of the discontinuity cancels itself after two revolutions (fig. 11(a)). For the field-free inhomogeneity, however, no such cancellation and suppression occurs. (fig. 11b). It may be noticed that the essential difference is that in fig. 11(b) the effect of the inhomogeneity (an added displacement) depends in sign upon the sign of the derivative of the orbit on encountering the inhomogeneity; in fig. 11(a), on the other hand, the effect of the inhomogeneity (an added derivative) is constant. The main resonances, for Q integral, do however occur in each case (fig. 11 c and d).

The stable regions for the field-free inhomogeneity are separated by bands of true instability, not merely lines of instability as was the case for the misalignment inhomogeneity. The reality of these 'stop-bands' (using the term common in filter-theory) is clearly seen (e.g. for a main resonance) by comparing fig. 11(d) and 11(e) which show the orbits at the limits of the instability band. A limit between a focussing orbit (sinusoidal envelope of oscillations) and a defocussing one (exponential envelope of oscillations) must clearly be an orbit whose amplitude increases linearly with revolutions, as has already been mentioned in Section 3 and two such orbits are drawn: figure 11(d) shows an orbit whose displacement at the centre of the straight section increases linearly and figure 11(e) shows an orbit whose slope at the centre increases linearly. Inspection of these two orbits shows that the 'stop-band' width is very nearly equal to a fractional change of wavelength given by

$$\frac{\Delta\lambda}{\lambda} = \frac{\delta}{Q\lambda} \quad \dots \quad (12)$$

where δ is the physical length of the field-free inhomogeneity. These 'stop bands' are, therefore, very narrow. If there are a number of random inhomogeneities in the circumference they can be represented, as before, by a single effective inhomogeneity of \sqrt{S} times the R.M.S. inhomogeneity, where S is the number of inhomogeneities.

As in the case of the misalignment inhomogeneity the amplitude of oscillation in the proximity of a stopband is finite, and stable but large. The 'forbidden band' in which amplitudes exceed the donut walls is therefore larger than the stop band.

To summarise, the main difference between the effects of a misalignment and a field free inhomogeneity is that, for the latter, the closed orbit always remains at the centre of the donut but the focussing oscillations about it become unstable in the stop bands, whereas, for the former, the closed orbit becomes unstable at the resonances while the focussing oscillations about it are unaffected by resonances. The misalignments must be reduced until there is room everywhere between the closed orbit and the donut wall for the unavoidable oscillations of particles about the closed orbit, and the stop bands must not be approached so near that the oscillation amplitude exceeds the donut dimensions.

These two quite different types of inhomogeneity have been chosen as particularly simple illustrative examples. Some more general types of inhomogeneity are shown in the table of fig. 12 and an analysis of them suggests the following method of classification of inhomogeneities²⁶; the classification relies on replacing the discontinuity by an equivalent discontinuity at the centre-point of the inhomogeneity.

* Since this lecture was given Sturrock has called attention to the possibility that resonances can be excited by twist inhomogeneities.

- (a) The orbit may be operated on, at a particular point of the circumference, by the addition of a constant displacement or derivative. An example of adding a constant derivative is the misalignment inhomogeneity (figs. 7 to 9, 11a and 11c). The effects of adding a constant displacement are very similar.
- (b) A displacement or derivative may be added which is proportional to the derivative or displacement of the orbit at the point where the inhomogeneity is applied. The field-free sector has been studied as the simplest type of such an inhomogeneity (fig. 10, 11(b), (d) and (e)); in it a displacement is added which is proportional to the derivative. More important is the effect of irregularities in the n value of nominally identical sectors. Such an irregularity is very nearly equivalent to the addition of a derivative which is proportional to the displacement of the orbit at that point. The behaviour is similar in all ways to that of adding straight sectors. It is summarised for completeness in fig. 13. It is particularly instructive to compare fig. 13(a) with fig. 11(a).
- (c) A displacement or derivative may be added which is proportional to some power of the existing derivative or displacement. Such inhomogeneities have not been listed in the table, but may well occur in practice. They would excite further sub-resonances, e.g. those with Q one-third integral, and split the stability diagram still further.
- (d) In general inhomogeneities may be resolved into a large number of terms with corresponding mixtures of the effects mentioned in subdivisions (a), (b) and (c), as well as mixtures of the effects mentioned in each sub-division.

The above description has treated those inhomogeneities caused mainly by mechanical irregularities. The various orbit changes and the widths of the stable bands for given mechanical irregularities depend in rather a complicated manner on the value of n chosen for the machine; in addition the minimum mechanical irregularities attainable will also depend on ' n ' in a manner which cannot yet be predicted. The general tendency is for mechanical tolerances to require a fairly low value of n . Then a realistic variation of n can be tolerated during the acceleration cycle without too much danger of moving into a "forbidden band".

In addition to mechanical tolerance difficulties, however, various inhomogeneities of magnetic origin are possible. These are caused by remanent magnetism, eddy current, etc.. The effects can be considered as equivalent to the mechanical effects already considered but a given field inhomogeneity causes a disturbance whose effect is reduced by a factor proportional to n compared with the equivalent mechanical inhomogeneity. The factor n arises because the rate of change of field with radius is proportional to n . Machines of lower n value tend, therefore, to be increasingly susceptible to inhomogeneities of magnetic origin.

5. Conclusion

From the foregoing discussion it is apparent that practical considerations of achievable accuracies greatly affect the design of the strong focussing synchrotron and determine how high a value of n should be used, i.e. how much advantage should be taken of the strong focussing idea. The aperture required does not vary rapidly with the n value. The already slow ideal variation of equation (10) ($A \propto n^{-1/2}$) is modified by azimuthal inhomogeneity considerations to give a broad range of n values for which the aperture used is approximately a minimum. Plausible designs can be worked out with apertures under ± 10 cm. for machines of energy 30 GeV. with n values in the region 100 to 1000 and the effect of the various parameters may be seen from the accompanying table (fig. 14).

The table (Fig. 14) assumes certain given tolerances both mechanical and magnetic on the magnet sectors. Unfortunately it is not yet known whether the values used are practicable. Information is required on the mechanical and magnetic tolerances achievable in the manufacture and measurement of magnets with various n values and apertures, on the changes in n and in field inhomogeneities occurring during the acceleration cycle, on the minimum angular and energy spread obtainable from an injector of given aperture, and on many other factors. In addition radio-frequency acceleration must be considered; this problems have been studied but have been excluded from this lecture. The effects of the various parameters are not, however, critical. It is likely, therefore, that most of the parameters can be fixed once full calculations and measurements have been made on a typical design.

It may be observed that the lecture has been restricted to a study of orbits in magnetic fields which vary linearly with radius. Some non linearity in the fields will, of course, occur in practice. Such non-linearity is beneficial from some viewpoints and harmful from others; there is as yet little justification for using deliberately non-linear fields. Indeed instabilities have arisen in many computed orbits using certain non-linear fields. The limits on the linearity of the magnetic field across the aperture is illustrated by the following table which gives the tolerance within which 'n' must be kept to avoid known bad effects of non linearity involving cubic terms in the magnetic field law. (i.e. a restoring force of the form $y - ky^3$.)

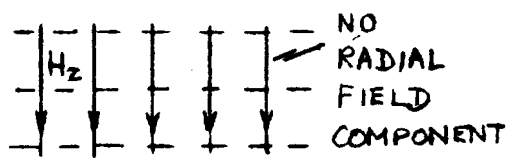
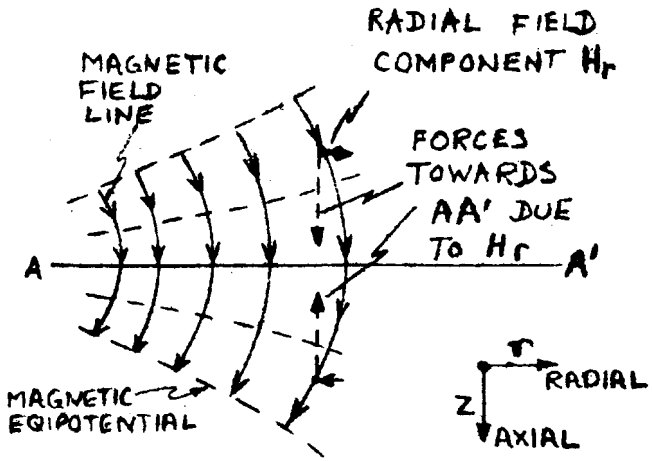
n	Tolerance $\frac{\Delta J}{J}$
3600	$\pm 1.7\%$
900	$\pm 3\%$
100	$\pm 10\%$

6. Appendix

This lecture was delivered on 21st May at Saclay and has been presented in written form at their request. It was considered desirable to add the arguments leading to equation (9), since these arguments crystallised to some extent during discussion at Saclay, and also to work out some physical explanation for 'stop-bands' by adding the section leading to equation (12.).

The lecture is based on work done in the C.E.R.N. proton synchrotron and theoretical groups, and in other laboratories and acknowledgement is made to information abstracted from many reports prepared for circulation inside C.E.R.N. A complete list of these reports and their authors is appended.

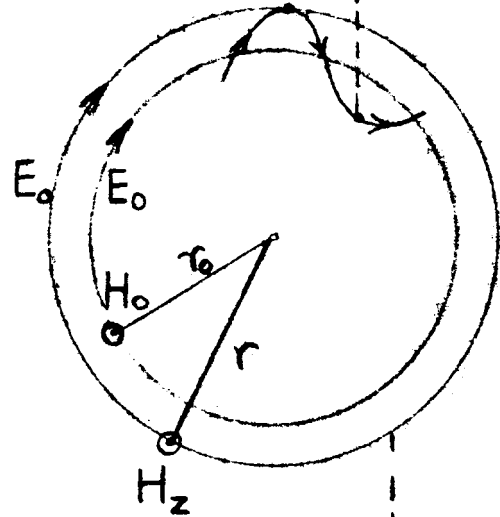
$H_z = H_0 (r/r_0)^{-n}$ WITH $n > 0$
 FOCUSING CONDITION



NEUTRAL EQUILIBRIUM
 IF $H_z = \text{CONSTANT}$
 i.e. $H_0 (r/r_0)^0$

$H_z = H_0 (r/r_0)^{-n}$ WITH $n < 1$
 FOCUSING CONDITION

FOCUSING REQUIRES FIELD TO BE:
 LARGE SMALL



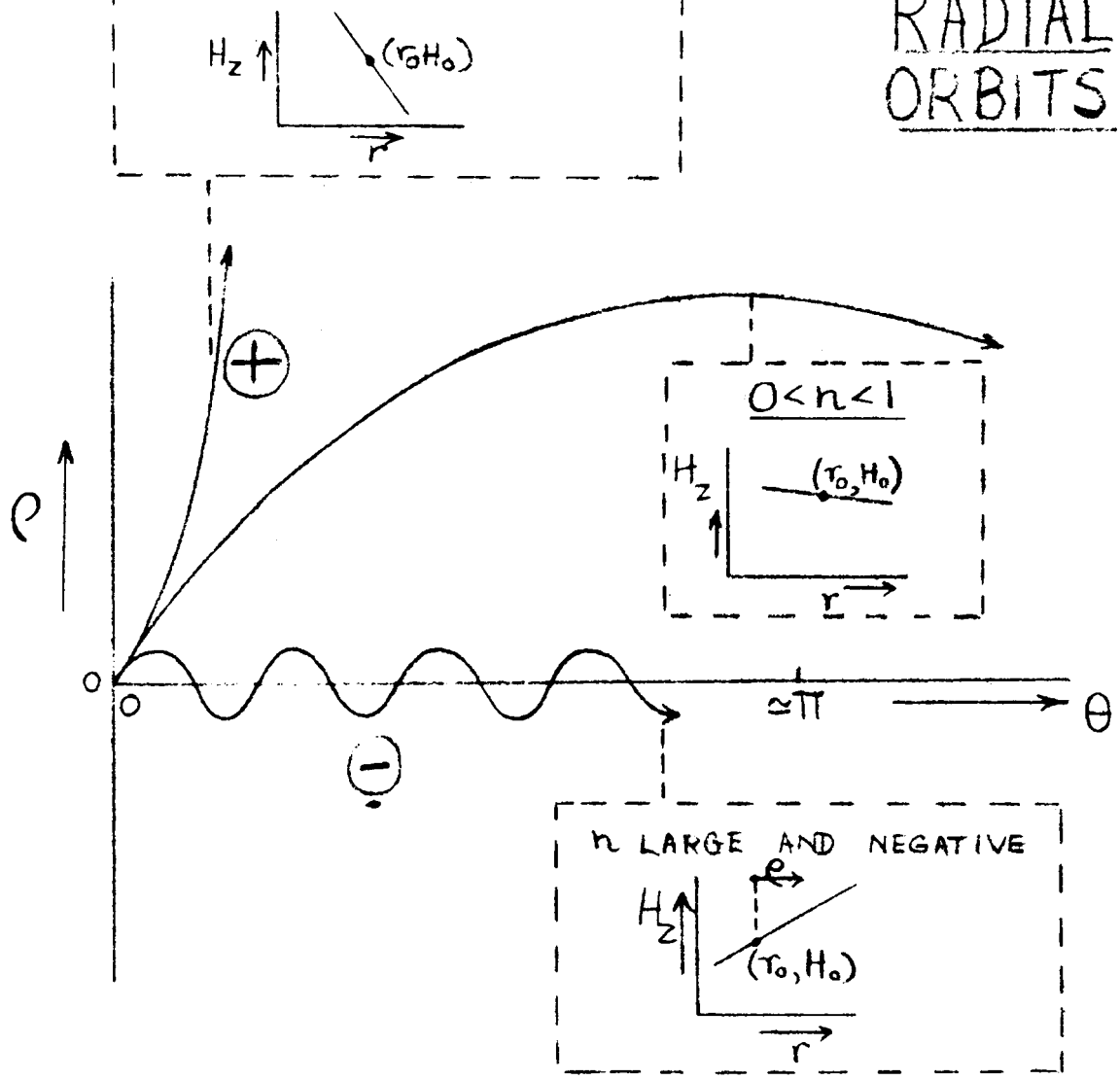
NEUTRAL EQUILIBRIUM
 IF $H_z r = H_0 r_0$ OR
 $H_z = H_0 (r/r_0)^{-1}$
 STABILITY LIMIT

FIG 1

COMBINED CONDITION FOR RADIAL AND AXIAL FOCUSING

$H_z = H_0 (r/r_0)^{-n}$ WITH $0 < n < 1$

RADIAL ORBITS



FOR RADIAL MOTION: $d^2\rho/d\theta^2 - n\rho = 0$

$\rho = a \cos \sqrt{-n} \theta + b \sin \sqrt{-n} \theta$

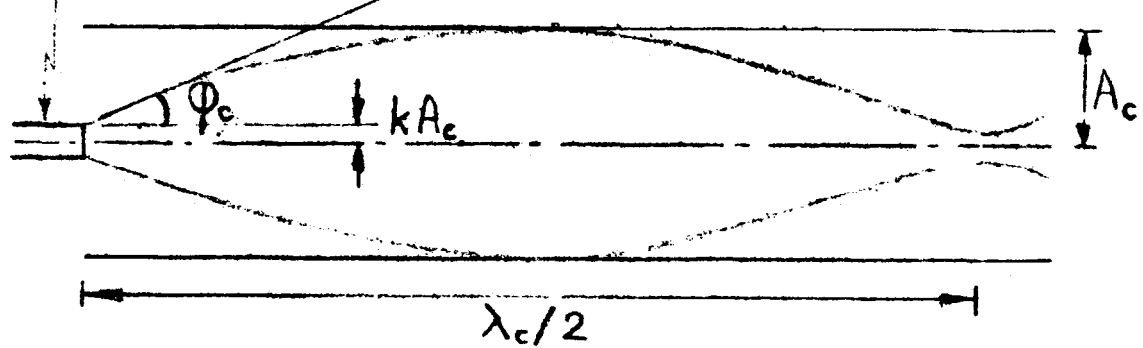
OSCILLATORY IF n IS NEGATIVE OR < 1 .

FOR AXIAL MOTION: $d^2z/d\theta^2 + nz = 0$

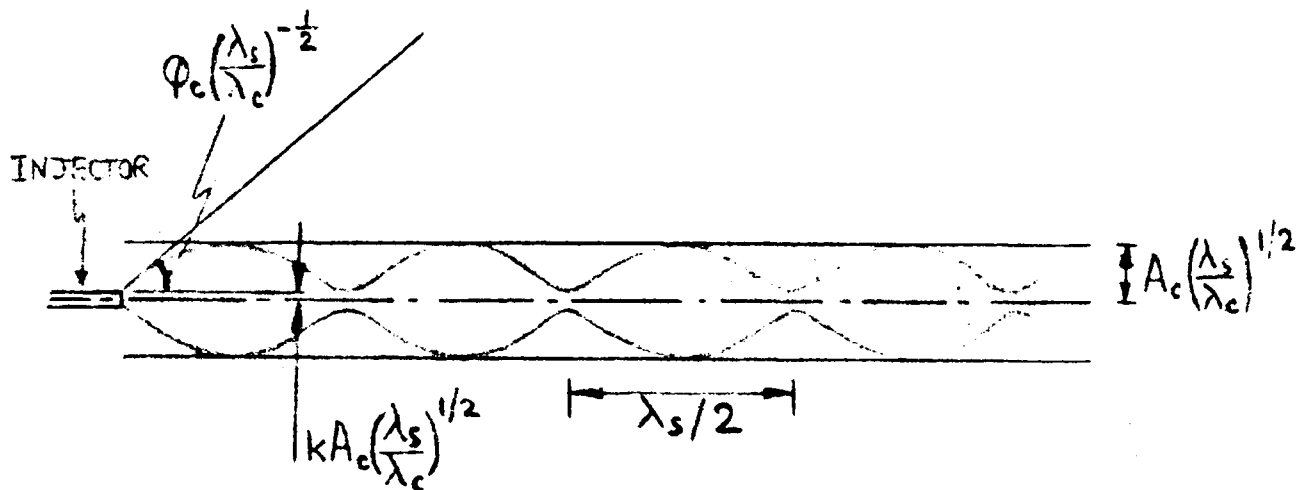
$z = a \cos \sqrt{n} \theta + b \sin \sqrt{n} \theta$

OSCILLATORY IF n IS POSITIVE

FIG 2 ORBITS IN HIGH-GRADIENT FIELDS



(a) CONVENTIONAL



(b) STRONG - FOCUSING

FIG 3: REDUCTION OF APERTURE AND INCREASE IN ANGULAR SPREAD FROM INJECTOR IN STRONG-FOCUSING SYNCHROTRON

NOTE:

ϕ_c , A_c AND λ_c ARE VALUES OF ϕ , A AND λ FOR CONVENTIONAL MACHINE. K IS A CONSTANT.

λ_s IS λ VALUE FOR STRONG FOCUSING MACHINE.

VALUES OF ϕ_s AND A_s SHOWN IN (b) ARE CONSISTENT WITH:

(1) $\phi \lambda / A = \text{CONSTANT}$

(2) INJECTOR DIMENSION $\times \phi = \text{CONSTANT}$

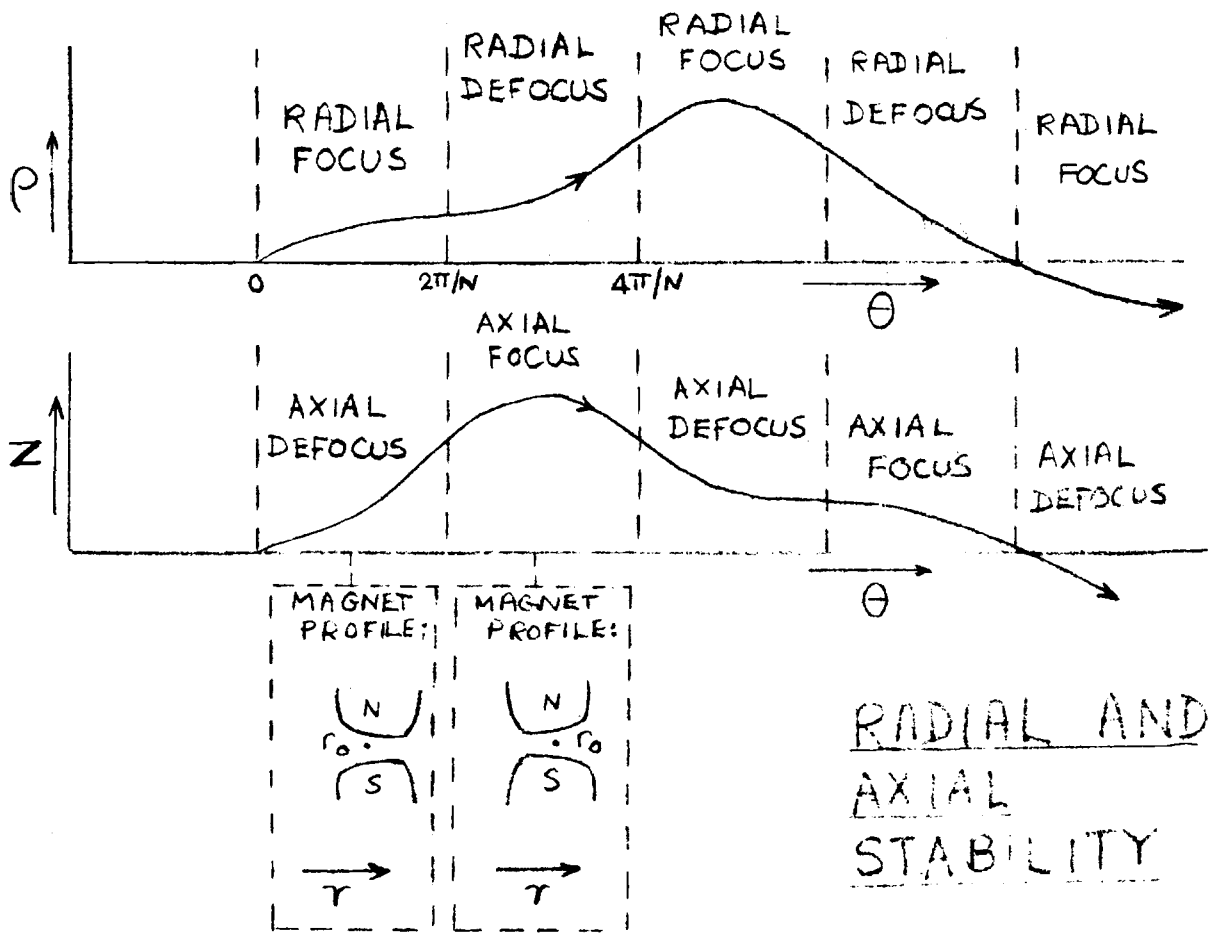
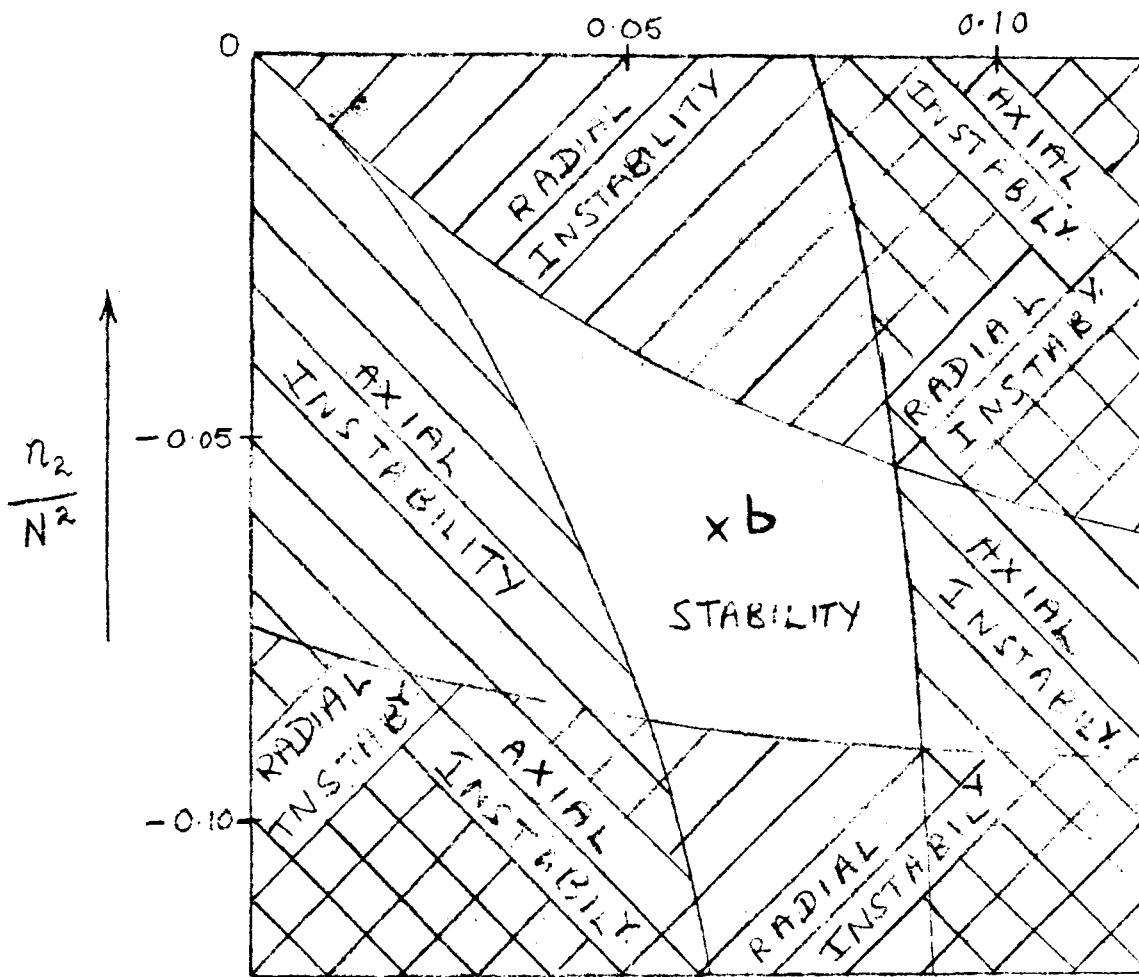


FIG 4 ORBITS FOR $\pi/2$ MODE IN STRONG FOCUSING SYNCHROTRON



n_1 IS n VALUE FOR NEGATIVE GRADIENT, OR AXIALLY FOCUSING SECTORS

n_2 IS n VALUE FOR POSITIVE GRADIENT, OR RADIALLY FOCUSING, SECTORS

N IS TOTAL NUMBER OF SECTORS

b SHOWS CONDITION $n_1 = -n_2 = N^2/16$

FIG 5: STABILITY DIAGRAM WITH NO AZIMUTHAL INHOMOGENITIES

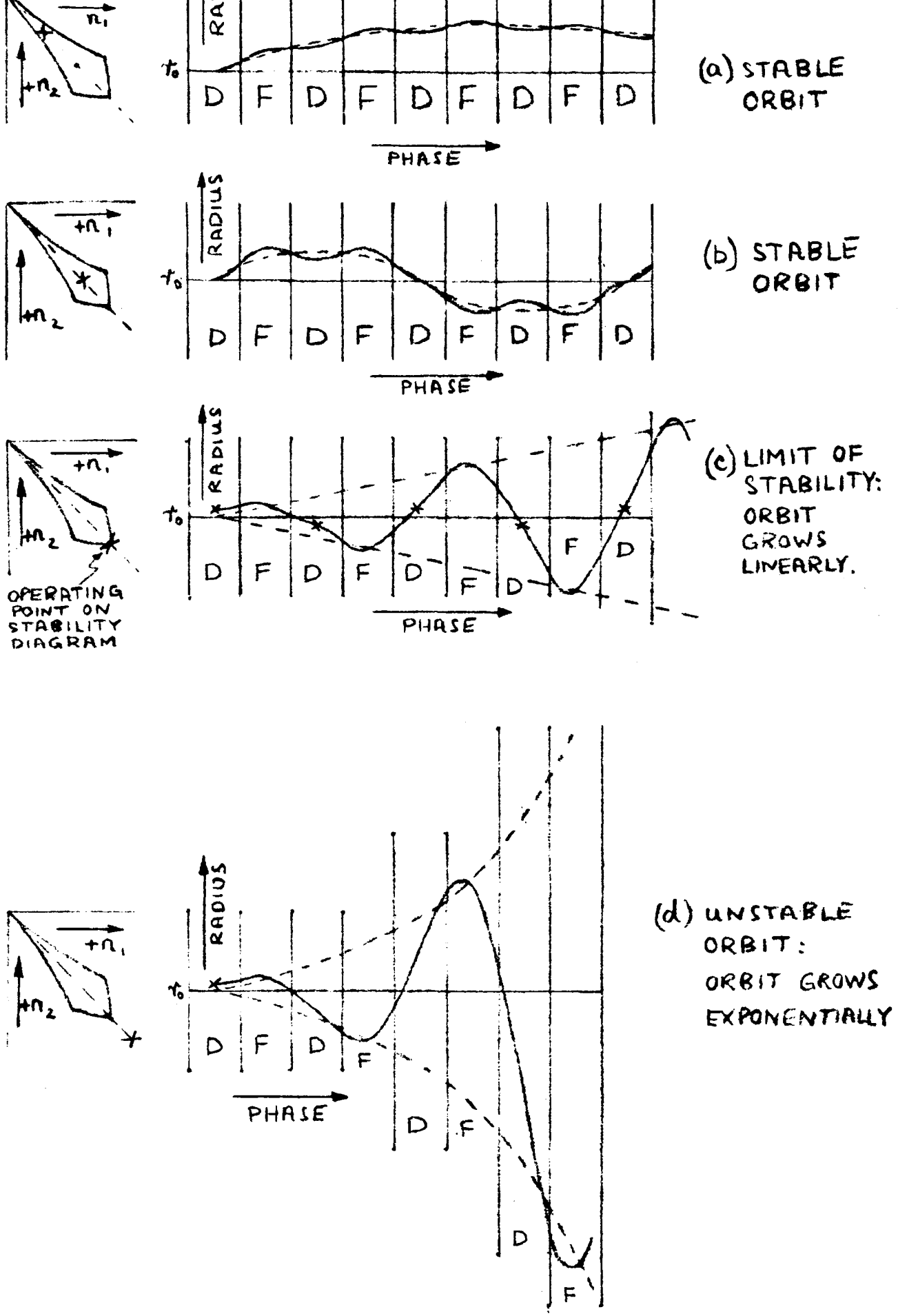
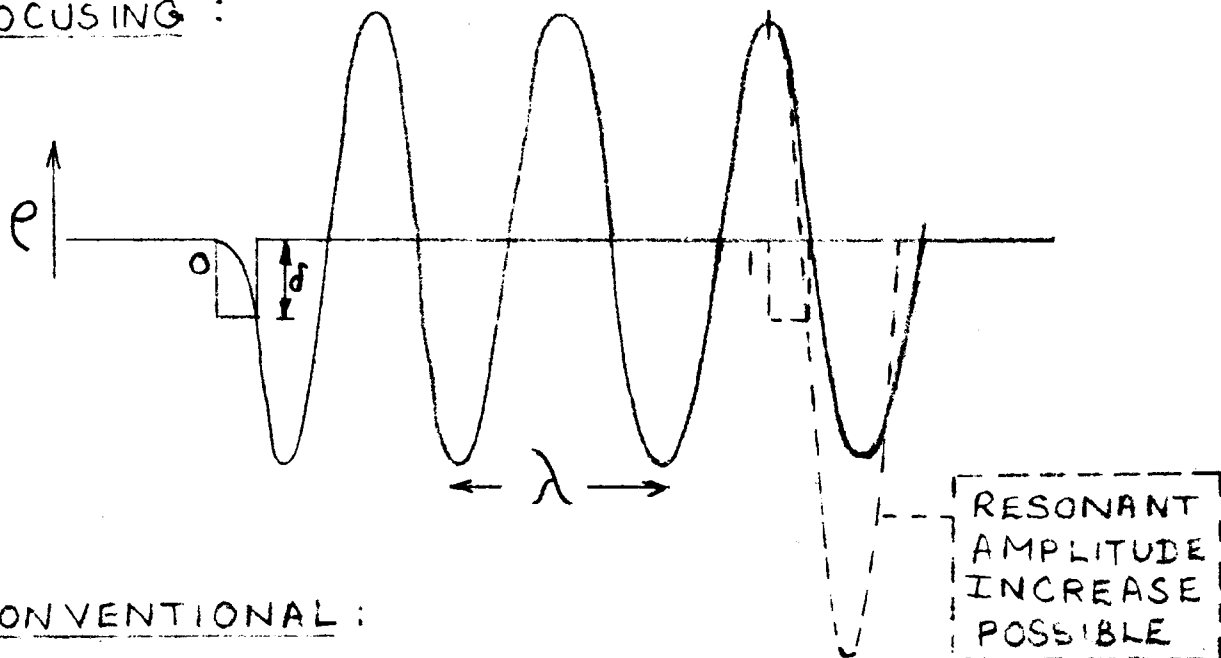


FIG. 6

DIAGRAM SHOWING ORBITS CORRESPONDING TO VARIOUS POSITIONS ON STABILITY DIAGRAM

STRONG-
FOCUSING :



CONVENTIONAL :

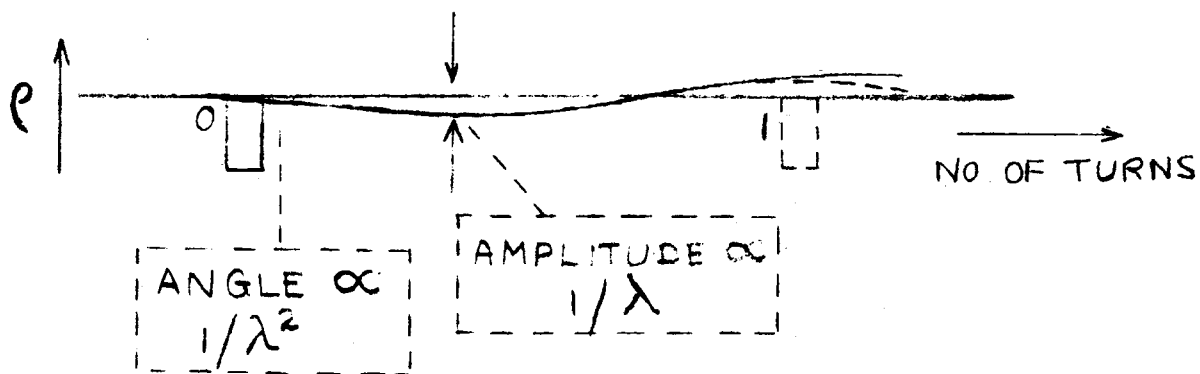
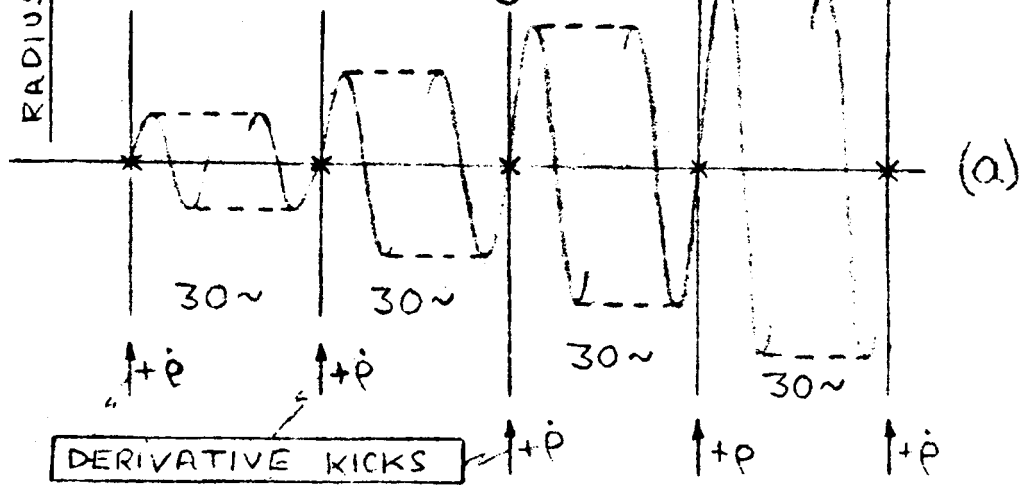
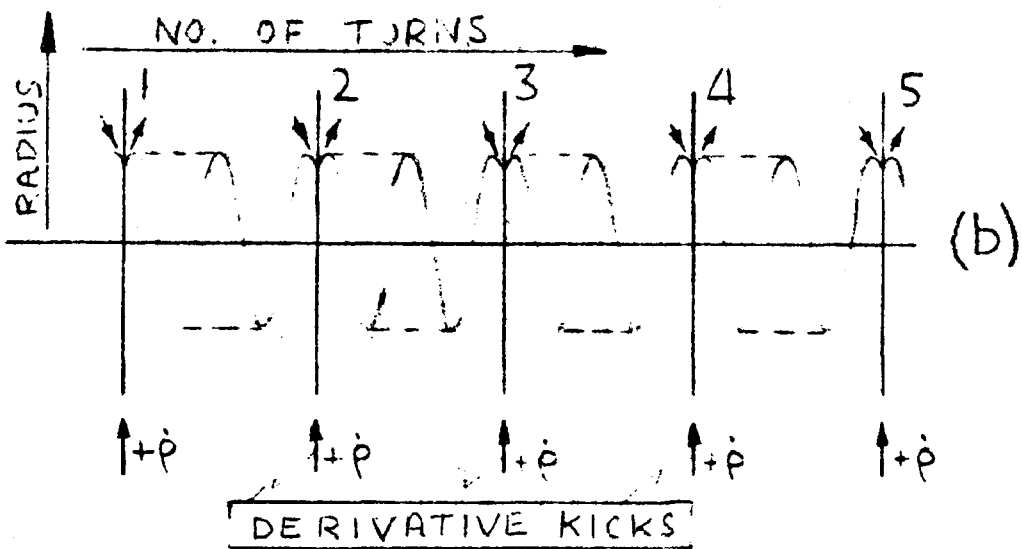


FIG. 7 :

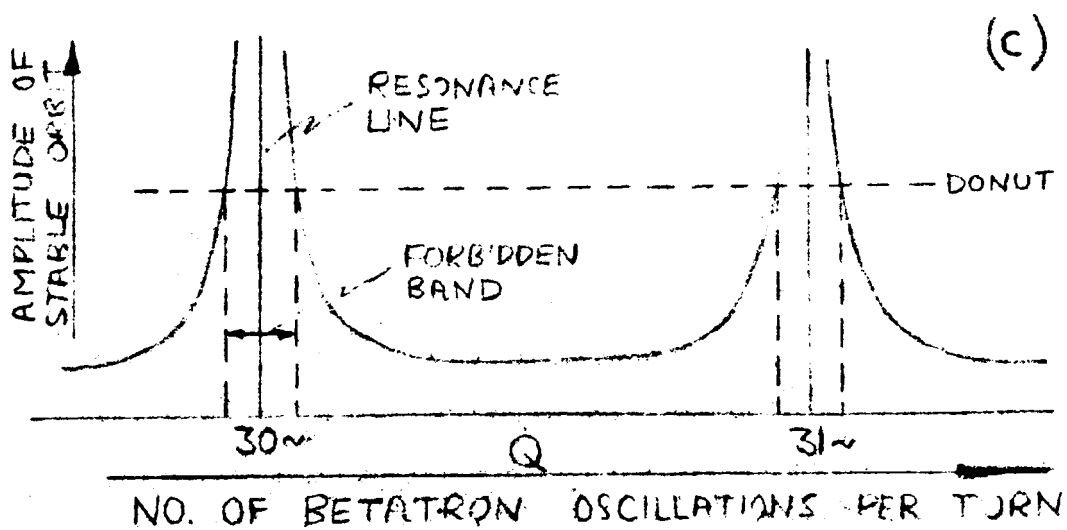
DISADVANTAGE OF STRONG-FOCUSING SYNCHROTRON IS ITS SENSITIVITY TO FIELD IRREGULARITIES



(a) RESONANCE



(b) STABLE ORBIT



(c) STABLE ORBIT AMPLITUDE VARIATION

FIG 8 SYSTEM WITH CONSTANT DERIVATIVE

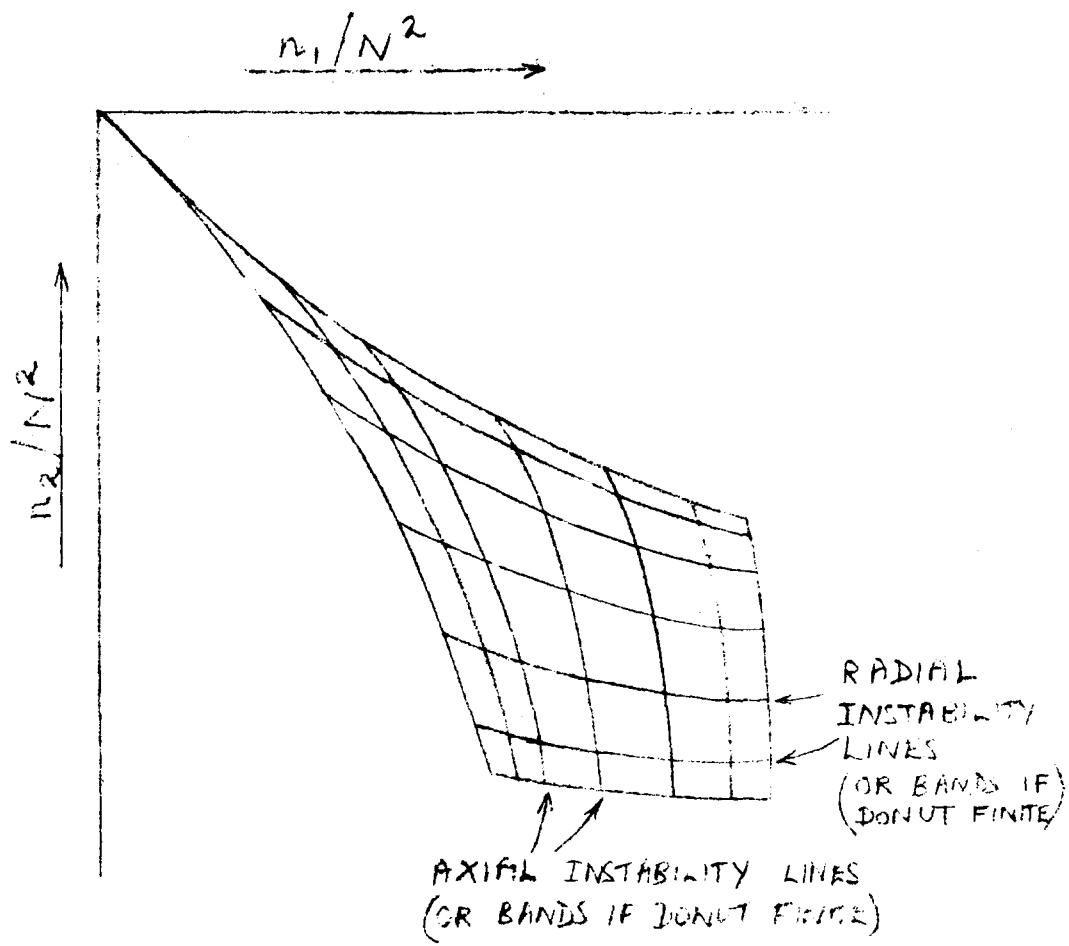


FIG. 9: STABILITY DIAGRAM IF CNR PERTURBATION
EACH REVOLUTION ADDS A CONSTANT
SLOPE

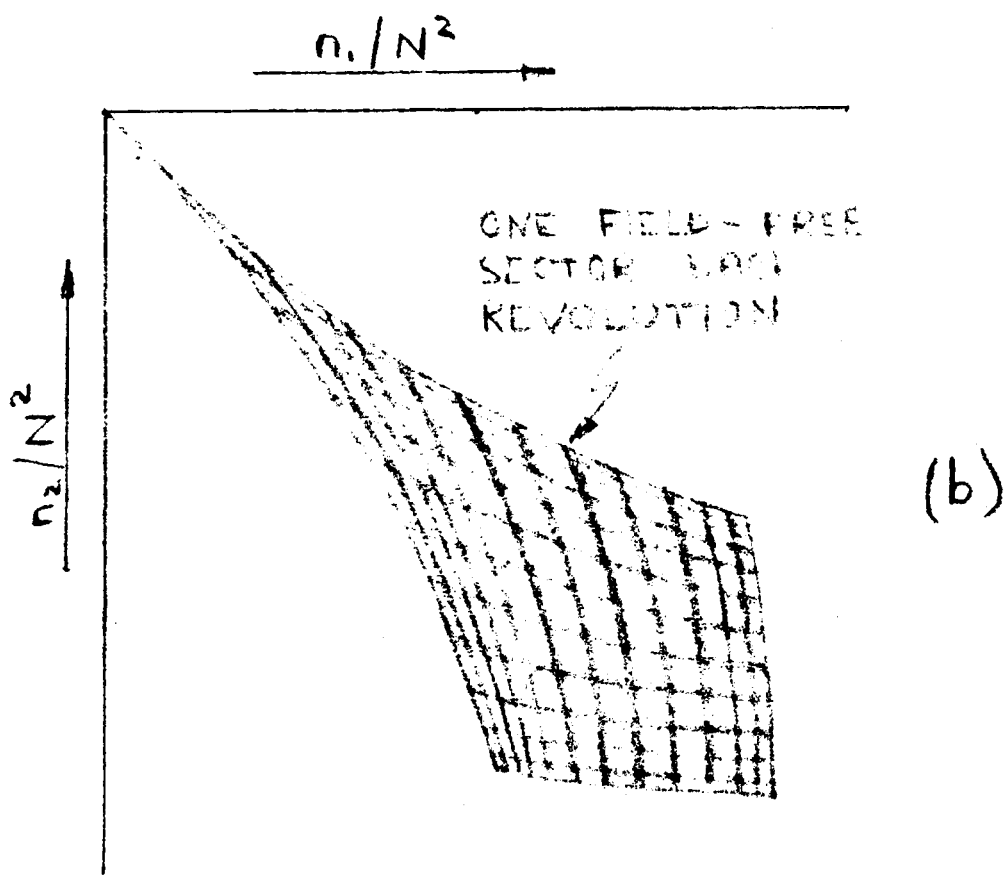
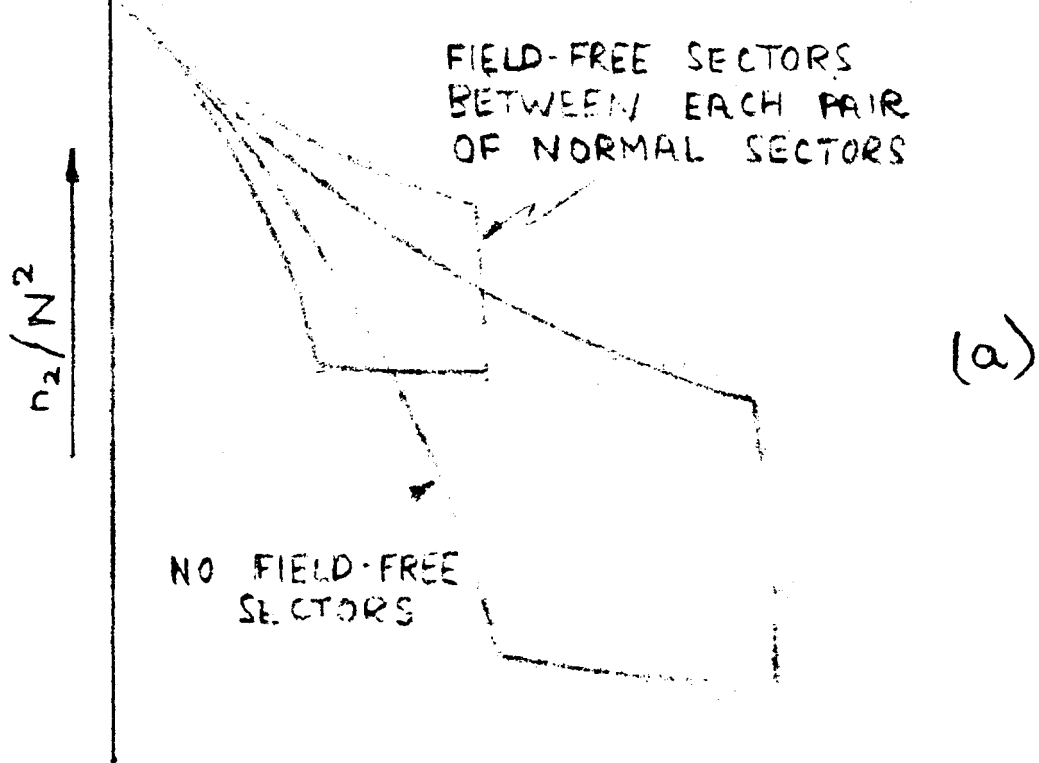


FIGURE: STABILITY DIAGRAMS WITH FIELD-FREE SECTORS

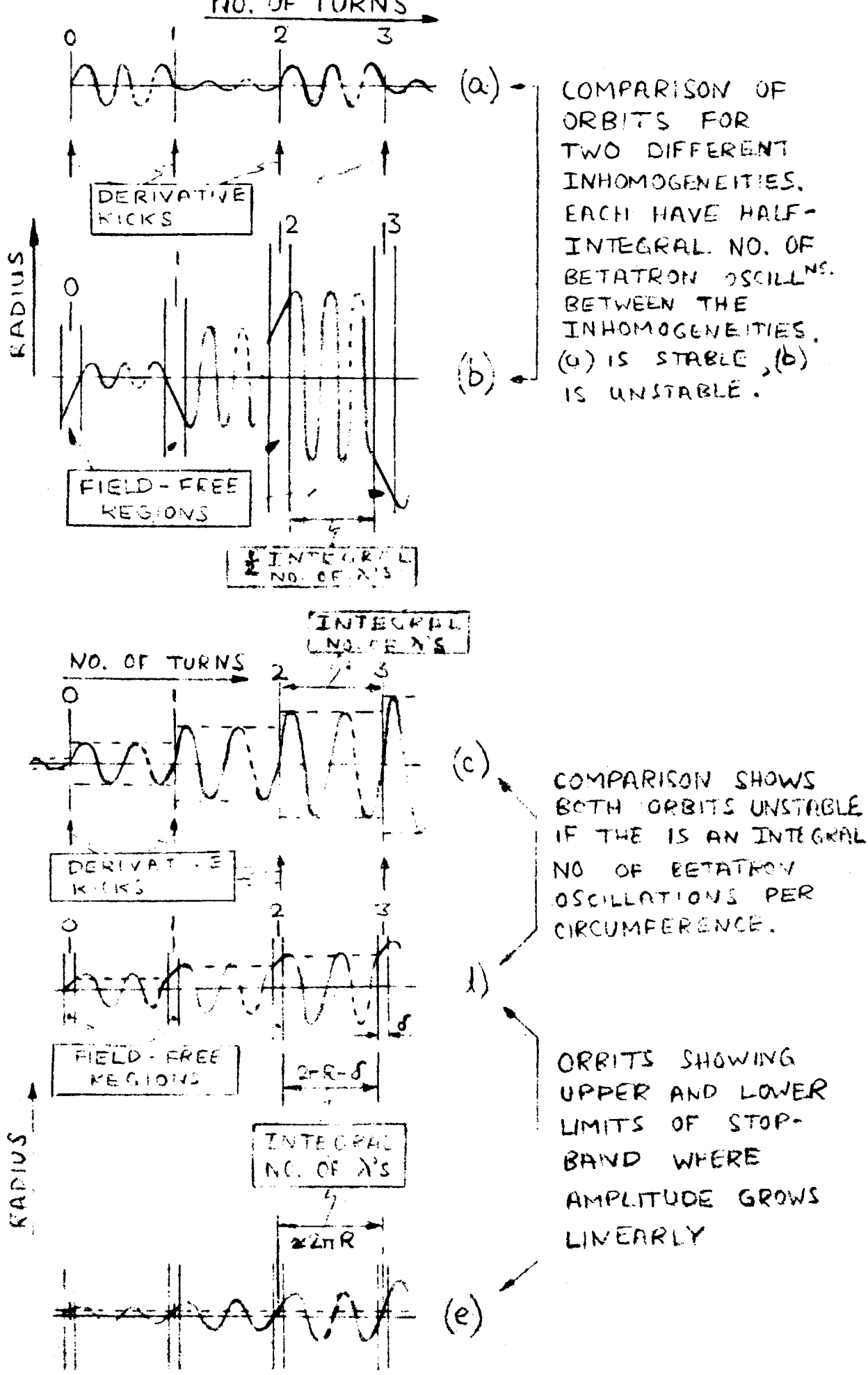
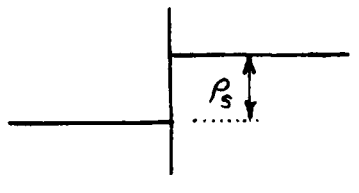
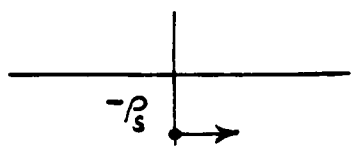
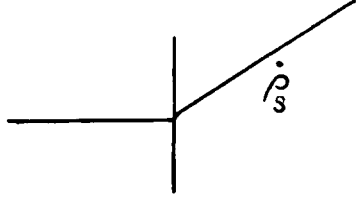
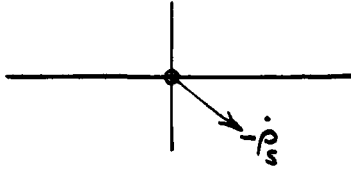
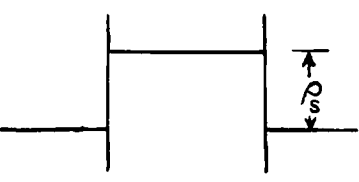
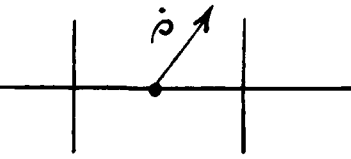
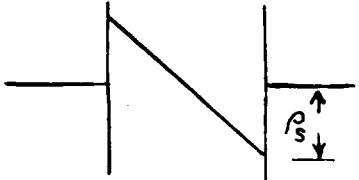
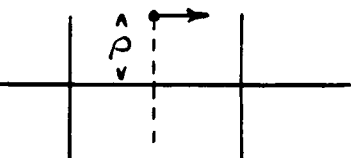
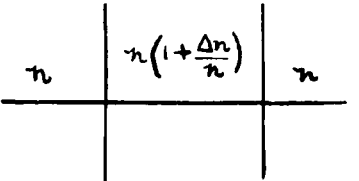
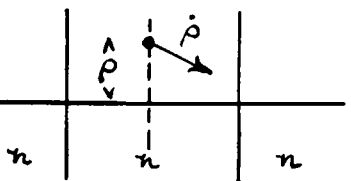
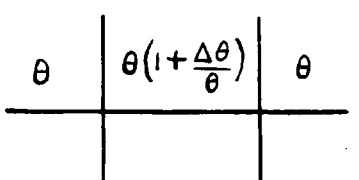
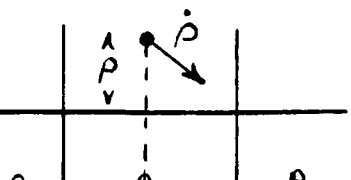
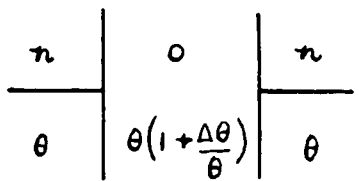
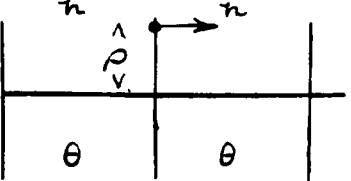


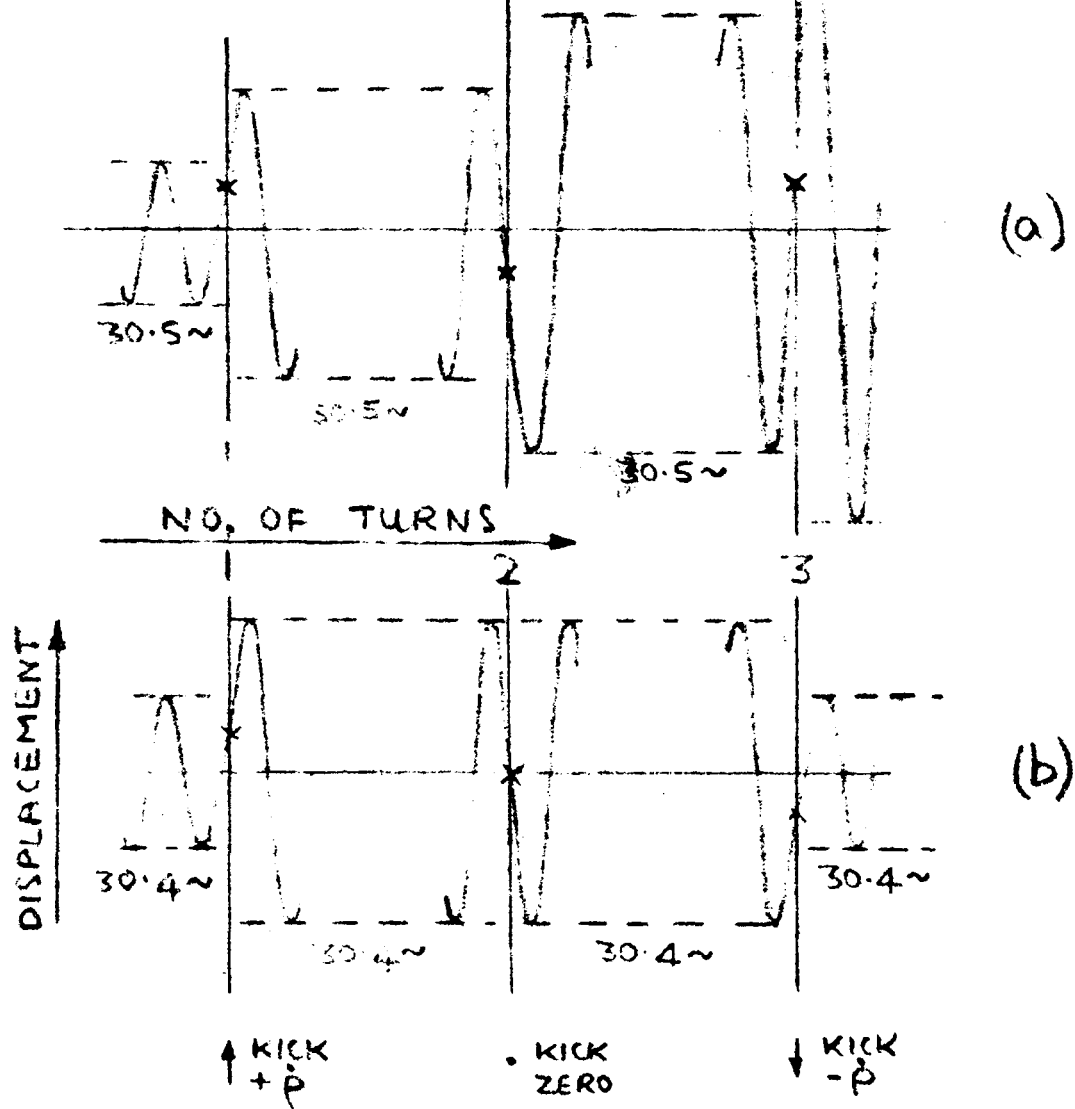
FIG. 11

ORBITS AT STOP BANDS.

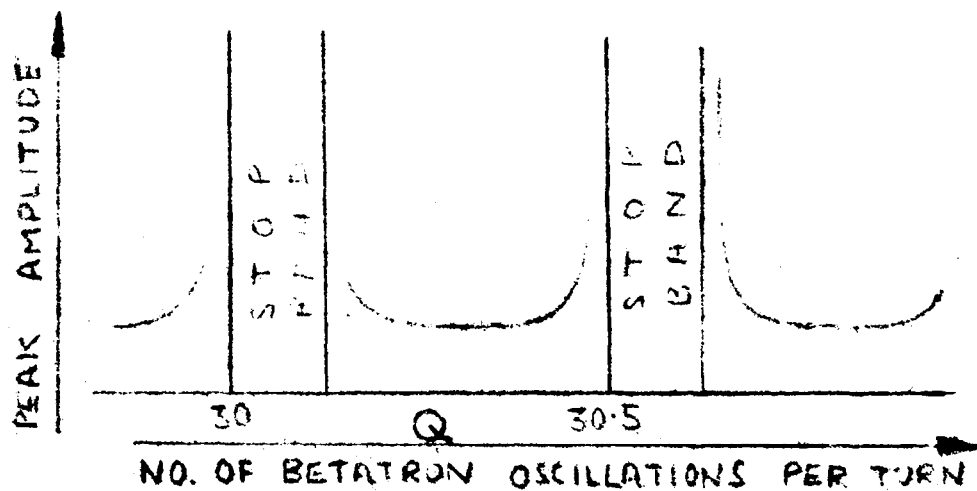
(a) and (b) SHOW "SUB-RESONANCE"

$\pi/2$ MODE

TYPE OF ERROR	RESULTING PERTURBATION	EQUIVALENT PERTURBATION AT THE CENTRE OF A PERFECT FOCUSING SECTOR.
DISPLACEMENT OF EQUILIBRIUM ORBIT AT A POINT		 $\rho = -\rho_s$
TILT OF EQUILIBRIUM ORBIT AT A POINT		 $\frac{\dot{\rho}}{\sqrt{n}} = -\frac{\dot{\rho}_s}{\sqrt{n}}$
DISPLACEMENT OF EQUILIBRIUM ORBIT IN ONE SECTOR		 $\frac{\dot{\rho}}{\sqrt{n}} = 1.414 \rho_s$
TILT OF EQUILIBRIUM ORBIT IN ONE SECTOR.		 $\rho = 3.86 \rho_s$
INCORRECT 'n' VALUE IN ONE SECTOR.		 $\rho = 0.285 \frac{\dot{\rho}_0}{\sqrt{n}} \cdot \frac{\Delta n}{n}$ $\frac{\dot{\rho}}{\sqrt{n}} = -1.285 \rho_0 \frac{\Delta n}{n}$
INCORRECT LENGTH OF ONE SECTOR		 $\rho = 1.571 \frac{\dot{\rho}_0}{\sqrt{n}} \cdot \frac{\Delta \theta}{\theta}$ $\frac{\dot{\rho}}{\sqrt{n}} = -1.571 \rho_0 \cdot \frac{\Delta \theta}{\theta}$
A FIELD FREE SECTOR BETWEEN NORMAL SECTORS		 $\rho = \frac{\pi}{2} \left(1 + \frac{\Delta \theta}{\theta}\right) \frac{\dot{\rho}_0}{\sqrt{n}}$



ORBIT PLOTS (a) AT EDGE OF STOP-BAND
SHOWING LINEAR GROWTH (b) AWAY FROM
STOP-BAND SHOWING OSCILLATORY ORBIT



STOP-BANDS AT MAIN AND SUB RESONANCE

FIG 13 SYSTEM WITH DERIVATIVE KICKS

FIG. 14. TABLE OF MACHINE PARAMETERS

Magnetic Field Index	n		3670	930	110	117
Phase shift per pair of sectors	μ		$\pi/2$	$\pi/2$	$\pi/2$	$\pi/5$
Betatron cycles per revolution	Q	$\propto n^{1/2}$	30.25	15.25	5.25	3.26
Magnet sectors per revolution	N	$\propto n^{1/2}$	242	122	42	66
Separation of main resonances	$\frac{\Delta n_1}{n} \%$	$\propto n^{-1/2}$	2.59	5.15	15.0	28.7
Separation of main resonance and adjacent sub-resonance	$\frac{\Delta n_2}{n} \%$	$\propto n^{-1/2}$	1.30	2.58	7.50	14.4
The stop band width caused by a) Random 1% variation in sector n-value	$\frac{2\Delta n_3}{\Delta n_2} \%$	$\propto n^{1/4}$	22.2	15.8	9.3	8.9
b) Random 0.2% variation in sector lengths	$\frac{2\Delta n_4}{\Delta n_2}$	$\propto n^{1/4}$	5.5	3.9	2.3	2.2
Final tolerance on n to avoid resonances and stop bands. (This is a maximum tolerance and in practice the working tolerance will be less than a half this value).	$\frac{\Delta n_5}{n}$		0.75	1.76	6.11	11.84
Vacuum chamber aperture	$\pm a$ cms	$\propto n^{-1/4}$	± 2.73	± 4.0	± 7.0	± 7.0
Variation in magnetic field across aperture for centre field of 10 KG.	ΔB in KG.		± 10	± 3.74	± 0.77	± 0.82
R.m.s. displacement of equilibrium orbit due to random remanent fields of $\sqrt{\Delta B^2}/B_0 = 1\%$ at injection	$\sqrt{\frac{\Delta R^2}{\text{cms}}}$		0.0272	0.0471	0.235	0.270
(The sectors are divided into elements of roughly constant weight)						
RMS betatron oscillation amplitude after one revolution due to,						
a) Mechanical errors $\sqrt{\Delta R^2} = 0.05$ cms.	%		62.5	40	13.5	14.2
b) Remanent fields $\sqrt{\Delta R^2}$	%		45	38	63	77
Synchrotron Oscillation amplitude, for injection energy of 50 MeV and 50th harmonic, as % of aperture	%		-	2.3	12.6	31